Electronic Supplementary Material (ESI) for Journal of Materials Chemistry B.

Supporting Information

Hetero-nanostructures of magnetic and antifungal nanoparticles as a platform for Magnetomechanical stress induction in *Saccharomyces cerevisiae*

K. Giannousi,[a] M. Menelaou,[a] J. Arvanitidis,[b] M. Angelakeris,[b] A. Pantazaki[c] & C. Dendrinou-Samara[a*]

[a]Lab of Inorganic Chemistry, Department of Chemistry, Aristotle University of Thessaloniki, 54124 Thessaloniki, Greece; [b]Department of Physics, Aristotle University of Thessaloniki, Thessaloniki, Greece; [c]Lab of Biochemistry, Department of Chemistry, Aristotle University of Thessaloniki

*Corresponding author: e-mail: samkat@chem.auth.gr

The crystal structures of the building NPs as well as NCs were verified by their XRD patterns (Fig. S1). The primary NPs are phase pure with the $NiFe_2O_4$ NPs exhibiting the cubic spinel structure (Fd3m) (JCPDS Card No. 10-0325), corresponding to the (220), (311), (222), (400), (422), (511), and (440) reflections and the Cu_2O NPs the cubic structure (Pn3m) of the (JCPDS Card No. 05-0667), corresponding to the (110), (111), (200), and (220) reflections. The NCs exhibiting reflections corresponding to both $NiFe_2O_4$ and Cu_2O phase. The crystallite sizes of the single NPs were estimated using the Scherrer's formula; 9.5 nm for $NiFe_2O_4$@OAm and 30 nm for Cu_2O@OAm NPs.

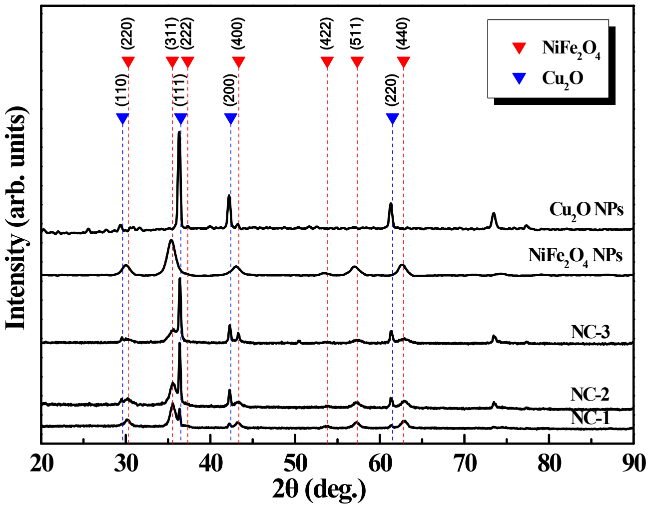

Fig. S1. XRD patterns of $NiFe_2O_4$ NPs, Cu_2O NPs, NC-1, NC-2 and NC-3.

The presence of OAm for the single nanoparticles as well as for the NCs was certified by FT-IR spectroscopy (Fig. S2). In all cases, the characteristic peaks are found shifted compared to pure OAm, as shown in Fig. S2. The peaks below 700 cm^{-1} are assigned to four vibrational modes (ν_1-ν_4) of the nickel ferrite structure (ν_1 and ν_2 modes are those with the highest frequencies and are due to the stretching vibration of the tetrahedral and octahedral sites) as well as to the Cu(I)-O bonds. In so, the vibrational modes occurring at ~625 cm^{-1} can be attributed to the overlapping of the metal-oxide bands of the nanocomposites (Cu(I)-O and ν_1) while the ν_2 band of the $NiFe_2O_4$ is detected at around ~400 cm^{-1} (marked by the dashed vertical line in Fig. S2).

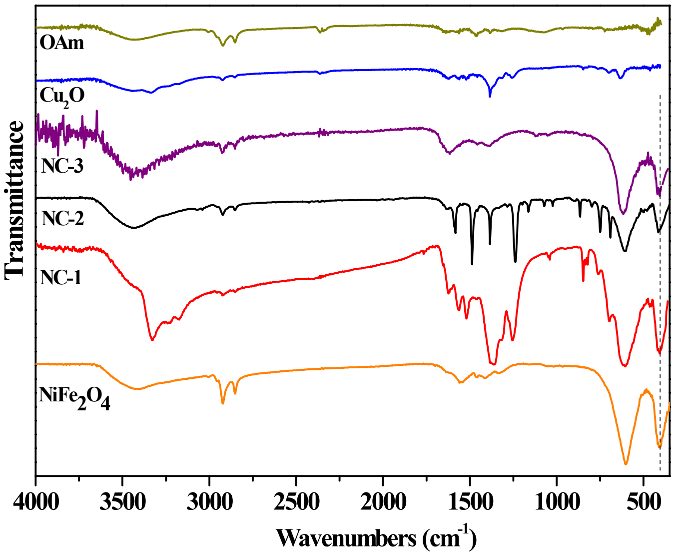

Fig. S2. FT-IR spectra of the OAm ligand, the -capped NiFe$_2$O$_4$@OAm and Cu$_2$O@ OAm NPs as well as of the isolated NCs (NC-1, NC-2 and NC-3). The dashed line demonstrates the absorption band corresponding to the ν_2 mode of the NiFe$_2$O$_4$.

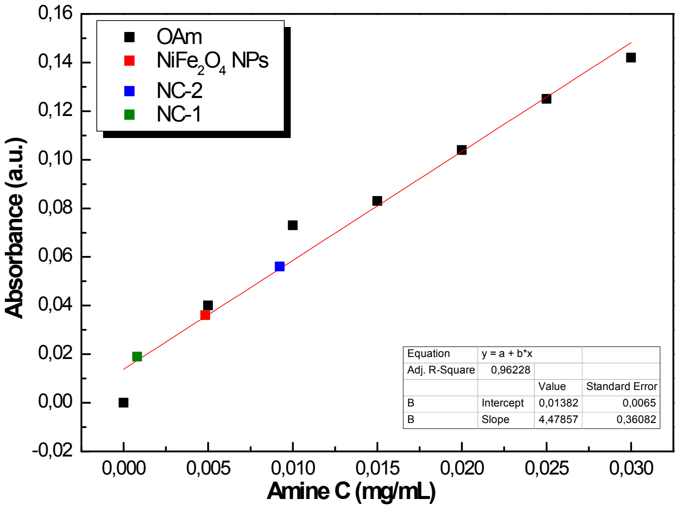

Fig. S3.Calculation of NH$_2$ groups based on the calibration curve prepared for OAm.

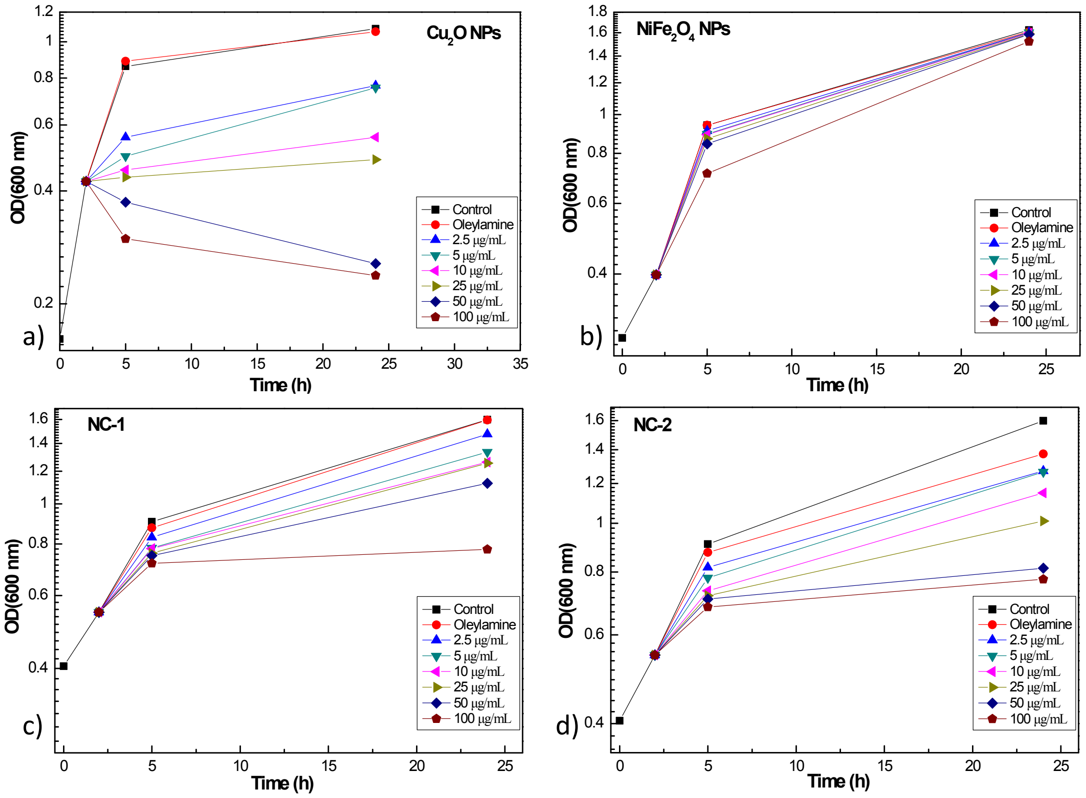

Fig. S4. Antifungal activity of (a) Cu_2O NPs, (b) $NiFe_2O_4$ NPs, (c) NC-1 and (d) NC-2 against yeast *S. cerevisiae* cells in the presence of 2.5 to 100 μg/mL of the NPs/NCs added at the logarithmic growth phase over 24 h. Fungal growth was measured as increase in absorbance at 600 nm.

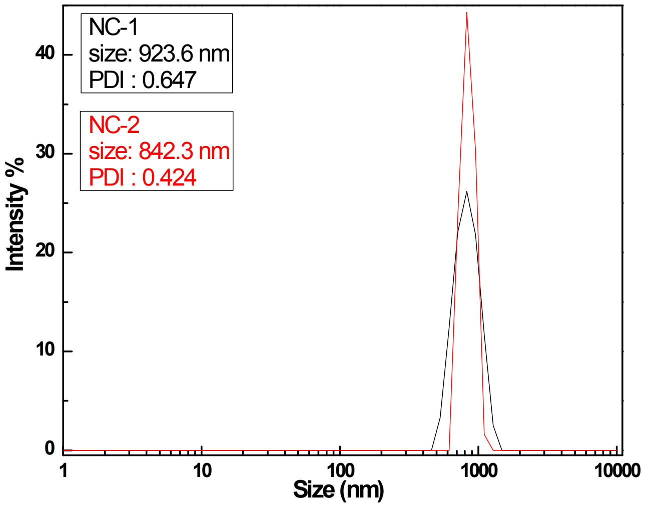

Fig. S5. DLS measurements of NC-1 and NC-2 in PBS.

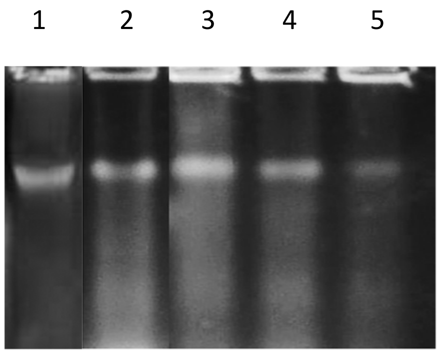

Fig. S6. *S. cerevisisae* genomic DNA fragmentation action of the NPs/NCs in agarose gel electrophoresis. Lane 1: control, DNA isolated from *S. cerevisiae* cells without incubated with NPs/NCs; Lane 2: DNA treated with 100 µg/mL of Cu_2O NPs; Lane 3: DNA treated with 100 µg/mL $NiFe_2O_4$ NPs after the exposure to the 30 Hz magnetic field; Lanes 4, 5: DNA treated with 100 µg/mL of NC-1 and NC-2, respectively after the exposure to the 30 Hz magnetic field.